Received: 27 September 2020 | Revised: 2 December 2020 | Accepted: 29 December 2020

DOI: 10.1002/btpr.3122

RESEARCH ARTICLE

BIOTECHNOLOGY PROGRESS

Model-based workflow for scale-up of process strategies developed in miniaturized bioreactor systems

Lukas Arndt[1] | Vincent Wiegmann[2] | Kim B. Kuchemüller[1] | Frank Baganz[2] | Ralf Pörtner[1] | Johannes Möller[1]

[1]Hamburg University of Technology, Bioprocess and Biosystems Engineering, Hamburg, Germany

[2]University College London, The Advanced Centre for Biochemical Engineering, Department of Biochemical Engineering, London, UK

Correspondence
Johannes Möller, Hamburg University of Technology, Bioprocess and Biosystems Engineering, Hamburg, DE [Technische Universität Hamburg].
Email: johannes.moeller@tuhh.de

Funding information
Bundesministerium für Bildung und Forschung, Grant/Award Number: Grant 031B0577A

Abstract

Miniaturized bioreactor (MBR) systems are routinely used in the development of mammalian cell culture processes. However, scale-up of process strategies obtained in MBR- to larger scale is challenging due to mainly non-holistic scale-up approaches. In this study, a model-based workflow is introduced to quantify differences in the process dynamics between bioreactor scales and thus enable a more knowledge-driven scale-up. The workflow is applied to two case studies with antibody-producing Chinese hamster ovary cell lines. With the workflow, model parameter distributions are estimated first under consideration of experimental variability for different scales. Second, the obtained individual model parameter distributions are tested for statistical differences. In case of significant differences, model parametric distributions are transferred between the scales. In case study I, a fed-batch process in a microtiter plate (4 ml working volume) and lab-scale bioreactor (3750 ml working volume) was mathematically modeled and evaluated. No significant differences were identified for model parameter distributions reflecting process dynamics. Therefore, the microtiter plate can be applied as scale-down tool for the lab-scale bioreactor. In case study II, a fed-batch process in a 24-Deep-Well-Plate (2 ml working volume) and shake flask (40 ml working volume) with two feed media was investigated. Model parameter distributions showed significant differences. Thus, process strategies were mathematically transferred, and model predictions were simulated for a new shake flask culture setup and confirmed in validation experiments. Overall, the workflow enables a knowledge-driven evaluation of scale-up for a more efficient bioprocess design and optimization.

KEYWORDS
mathematical process models, model-assisted scale-up, Monte Carlo uncertainty analysis, quality by design

1 | INTRODUCTION

In the initial phase of bioprocess design and optimization, the identification of an appropriate process strategy (e.g., feeding design) can be demanding due to the large number of influencing factors.[1-3] To accelerate the optimization procedure, miniaturized bioreactors (MBRs) are typically applied in the field of mammalian cell culture processes with Chinese hamster ovary (CHO) cells. Advantages are a reduced

working volume (e.g., 1–2.5 ml in 24-Deep-Well-Plate—24-DWP) and increased automation and parallelization possibilities.[1,4-10] In the past, several research groups have demonstrated the potential of MBRs for the cultivation and optimization of mammalian producer cell lines.[1,11-14] However, the scale-up and scale-down of process understanding (i.e., knowledge) between MBR systems and benchtop- or production-scale can be challenging due to varying process performance and cellular changes.[15-17] Nowadays, scientific methods are increasingly applied to ensure process stability during scale-up, taking the Quality by Design (QbD) methodology into account.[6,15,18-20] QbD demands the implementation of a knowledge-based workflow, which can be used to understand the impact of critical process parameters on the process performance.[15,16,20,21] If purely data-driven approaches are used in the knowledge-based workflow, the dynamics of cell growth, metabolism and productivity are mostly not sufficiently considered and quantified.[15]

To enable a more knowledge-driven decision making, mathematical process models can be combined with statistical tools to further reduce the experimental effort and to understand the complexity and dynamics of an existing bioprocess *in silico*.[3,22-26] Therefore, the mechanistics of the bioprocess are modeled in different bioreactor scales and with varying process strategies (e.g., fed-batch). Additional process knowledge is gained if effects of input uncertainties (e.g., experimental variations) on model outcomes are considered and quantified (e.g., using Monte-Carlo methods).[15,27] By this, biological variability and fluctuations inherent in bioprocesses are incorporated into the model and model parameter distributions.[23,28] Subsequently, individual model parameter distributions can be statistically compared to identify changes in the process dynamics between the modeled scales, as shown in Möller et al.[15] So far, this approach was successfully applied for the model uncertainty-based evaluation of an antibody-producing CHO process from shake flask cultures up to pilot scale. However, the scale-up of process strategies developed in rather undefined small scale MBR systems to mostly characterized larger scale remains challenging.[6]

In this study, a model-based scale-up methodology is introduced to evaluate and mathematically transfer the process dynamics from MBR to larger scale bioreactors (i.e., lab-scale). Therefore, model-parametric uncertainties are determined under consideration of

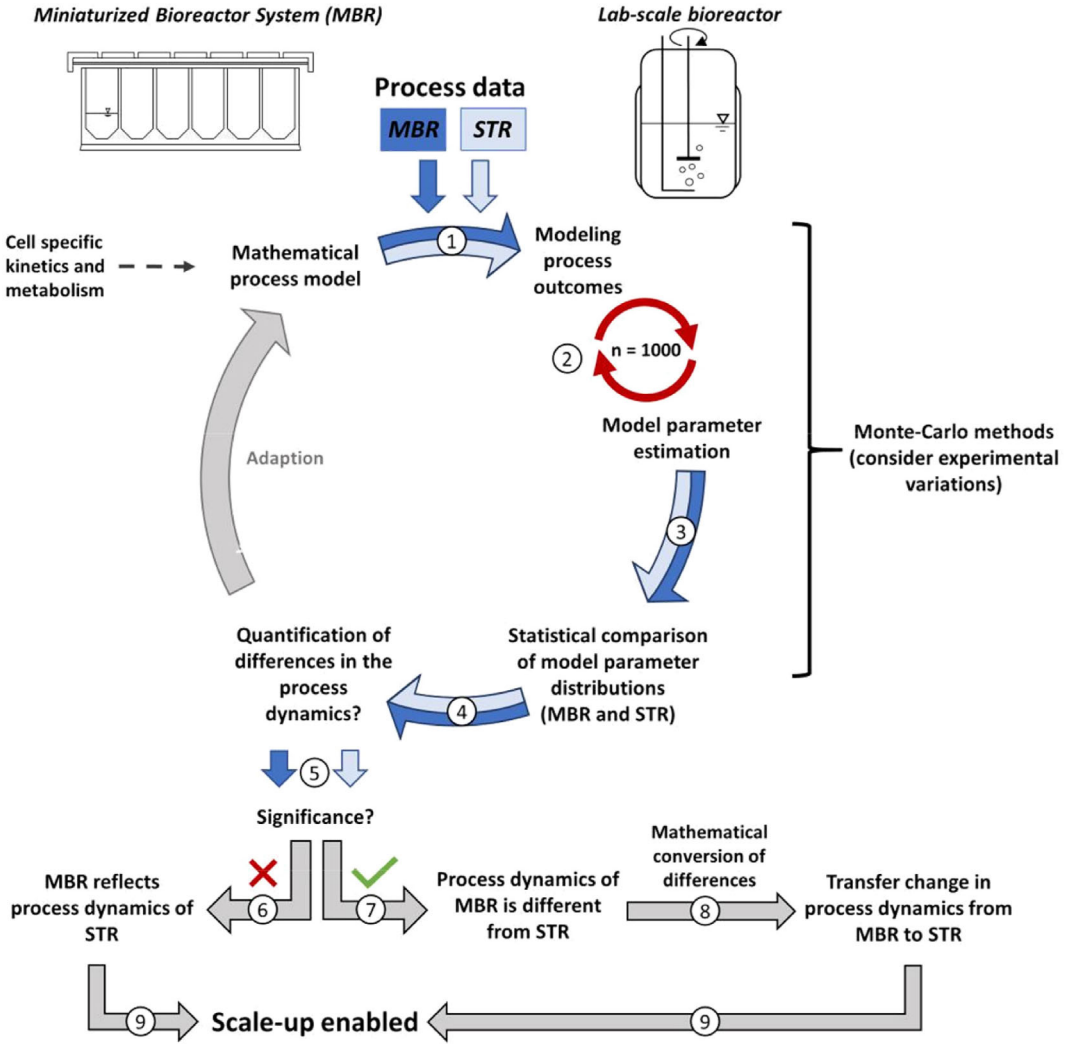

FIGURE 1 Model-based workflow for the scale-up of biotechnological processes

TABLE 1 Performed cultivations in CS1 and CS2

Aim	Number of cultivations	Working volume (cultivation system)
Process development	1	4 ml (micro-matrix, CS1)
Scale-up	1	2.5–3.75 L (BIOSTAT B-DCU, CS1)
Process development	8	2 ml (24-DWP, CS2)
Process development	4	30–50 ml (shake flask, CS2)
Validation	4	30–50 ml (shake flask, CS2)

experimental uncertainty in both investigated scales. This methodology is shown for two different case studies with antibody-producing CHO cells. In case study I (CS1), the methodology was applied to compare a fed-batch process (GS-CHO) between the micro-matrix system (4 ml working volume) and a stirred tank bioreactor (3750 ml working volume). In case study II (CS2), the process dynamics in a fed-batch process (CHO DP-12) with two different feeding media were compared between a 24-DWP system (2 ml working volume) and shake flask culture (40 ml working volume).

1.1 | Uncertainty-based workflow

In Figure 1, the suggested workflow for the model-assisted scale-up of process strategies from MBR to larger-scale bioreactors is shown.

Aim of this workflow is the quantification of differences in the process dynamics between MBR and larger-scale bioreactor systems. Initially, experimental cultivation data of two different bioreactor scales, for example, MBR and shake flask, are used to determine the model-parametric uncertainties based on the experimental variability (i.e., measurement errors). By this, the experimental variability in both biological cell behavior and measurements are considered. Therefore, the dynamics of the bioprocess are modeled (Figure 1 (1)) and the model parameters are adapted multiple times for each scale based on an assumed normally distributed measurement error of the experimental data (Figure 1 (2)).[15] For each scale, individual model parameter distributions are determined. In order to evaluate significant differences in the dynamics of the cultivations between different scales, the model parameter distributions are statistically compared (Figure 1 (3)). The differences are quantified (Figure 1 (4)) and tested for significance (Figure 1 (5)). The approach of statistical testing of model parameter distributions was derived from previous studies in the field of systems biology and are advantageous for bioprocess design and optimization since the process dynamics of the biological system are captured.[23,24] If no differences between both model parameter distributions are identified (Figure 1 (6)), the dynamics can be seen as comparable at both scales (process dynamics of small scale reflects the larger-scale) and the scale-up is evaluated successfully (Figure 1 (9)). Otherwise, if the model parameter distributions are different (Figure 1 (7)), a mathematical conversion of the parameter distributions between both scales is performed to convert the process dynamics from MBR to larger scale (Figure 1 (8)). Subsequently, the outcomes are validated by experiments at the larger scale. This methodology enables a model-assisted scale-up and validation of process strategies obtained in MBR systems for a more holistic process understanding (Figure 1 (9)).

2 | MATERIALS AND METHODS

2.1 | Cell line and preculture

2.1.1 | Antibody-producing GS-CHO (CS1)

An industrial glutamine synthetase CHO (GS-CHO) cell line (Lonza, UK) producing an IgG4 antibody was used in the CS1 experiments.[10] Cells were thawed and transferred to 49 ml of CD-CHO medium (Life Technologies, UK) containing 25 μmol L^{-1} methionine sulphoximine in a vented 250 ml shake flask (Corning Life Sciences, USA). Cells were expanded on an orbital shaker with 25 mm shaking diameter (Sartorius, UK) at 160 rpm, 37°C, 5% CO_2, 70% humidity and passaged every 3–4 days. The inoculum was prepared after 12–14 days of pre-expansion from cell populations in the exponential growth phase. The seeding density of all cultivations was 0.3×10^6 cells ml^{-1}.

2.1.2 | Antibody-producing CHO DP-12 (CS2)

CHO DP-12 cells (clone #1934, ATCC CRL-12445, kindly provided by T. Noll, Bielefeld University, Germany) producing an interleukin-8 antibody were used in CS2. The cell line was cultivated in animal component-free and chemically defined TC-42 medium (Xell AG, Germany). The medium was supplemented with 42 mmol L^{-1} of glucose, 6 mmol L^{-1} of glutamine and 200 nmol L^{-1} of methotrexate (all Sigma-Aldrich, Germany). One milliliter of cryoculture (10^7 cells ml^{-1}) was thawed and inoculated into a vented single-use shake flask (baffled, 40 ml working volume, Corning Life Sciences, USA) with 40 ml prewarmed medium. The incubator (Kuhner LT-X, Kuhner AG, Switzerland) conditions were set to 37°C temperature, 5% CO_2, and 85% humidity. The orbital shaker was set to a shaking frequency of 200 rpm with 25 mm shaking diameter.

2.2 | Fed-batch cultivations

The setups for all cultivations are summarized in Tables 1 and S1.

2.2.1 | Fed-batch cultivation in micro-matrix (CS1)

Prior to each experiment, each well of a micro-matrix (Applikon-Biotechnology, The Netherlands) was filled with 2 ml of 1×PBS (Life

Technologies, UK). The cassette was then covered with the micro-matrix feeding module and mounted onto the micro-matrix system. The pH was monitored for at least 2 h using the HMI software. The offset of the online pH was then corrected by comparison to the corresponding readings of an offline pH meter (Mettler Toledo, Switzerland). The inoculum was prepared by mixing prewarmed CD-CHO medium with the appropriate volume of cell broth to reach a cell density of 0.3×10^6 cells ml^{-1}. PBS was then removed and replaced with 4 ml of the inoculum. The liquid feed bottle was filled with 1 mol L^{-1} sodium hydroxide (Acros, Belgium) and all lines were primed before the cultivation commenced. The agitation speed was set to 250 rpm (25 mm orbit), pH was controlled at 7.2 using either overlay with carbon dioxide or automated base additions. The dissolved oxygen was controlled at 30% using either overlay of air or nitrogen. The temperature was controlled at 37°C. Feeding with Efficient Feed B (Life Technologies, UK) was performed after 3 days of cultivation and was repeated on Days 5, 7, 9, and 11 with bolus additions ranging between 286 and 400 µl to match the volumetric additions at the 5 L scale bioreactor.

2.2.2 | Fed-batch validation in 5 L scale (CS1)

Benchtop-scale cultivations were performed in a 5 L BIOSTAT B-DCU STR (B. Braun Biotech, Sartorius, UK), equipped with a 45-degree pitched blade impeller in down-pumping configuration. The rotational speed was set to 260 rpm and the vessel content was continuously aerated with 0.07 vvm via a ring sparger. The pH was controlled at 7.2 using either sparging of carbon dioxide or 1 mol L^{-1} sodium hydroxide additions. The DO was maintained at 30% by sparging either air or nitrogen. The temperature was controlled at 37°C and 1% Antifoam C Emulsion (Sigma-Aldrich, UK) was added as needed. Since Antifoam C is commonly used in cell culture processes, its impact on cell growth and metabolism was not focused in this study. Cells were seeded in equilibrated CD-CHO medium at a concentration of 0.3×10^6 cells ml^{-1} and cultivated in an initial working volume of 2,500 ml.

Feeding with 250 ml of Efficient Feed B commenced after 3 days of cultivation and was repeated on Days 5, 7, 9, and 11. All cultivations are described in Section 2.2 and are summarized in Table 1.

2.2.3 | Fed-batch cultivation in 24-DWP (CS2)

A re-usable squared-bottom 24-DWP (SMCR1424, Duetz System, Kuhner AG, Switzerland) with a working volume of 1–2.5 ml was used.[29] The 24-DWP was placed in an incubator (Kuhner LT-X, Kuhner AG, Switzerland) and mounted on a holder (SM318000, Kuhner AG, Switzerland). Cultivation conditions were set to 37°C, 5% CO_2, 85% humidity and 220 rpm with an orbitally shaking diameter of 25 mm. 0.3×10^6 cells ml^{-1} were inoculated in pre-warmed medium containing 42 mmol L^{-1} glucose, 6 mmol L^{-1} of glutamine and 200 nmol L^{-1} methotrexate (same medium as in Section 2.1). Every 24 h a sample of 200 µl was taken and directly diluted in 800 µl 1×PBS (Sigma-Aldrich, Germany). Two different constituted feed media were used for feeding. Among other differences, feed medium A contained 111 mmol L^{-1} glucose (Basic CHO feed, Xell AG), and feed medium B 222 mmol L^{-1} glucose (HEK FS feed, Xell AG). Both feed media (Feed A and Feed B) were supplemented with 9 mmol L^{-1} glutamine (Sigma-Aldrich, Germany). The set-ups for all cultivations in the 24-DWP with respect to feed volume, concentrations and initial time point are listed in Table S1.

2.2.4 | Fed-batch cultivation in shake flasks (CS2)

The shake flask cultivations were part of a previous publication, please see Möller et al.[3] Out of these data, four cultivations characterized by a feed concentration of 111 mmol L^{-1} glucose (Feed A), were selected. The glutamine concentration of the feed medium varied from 9 to 38 mmol L^{-1}. The feed concentrations and feeding time points varied for all cultivations (see Table S1).

2.3 | Mathematical process model

The cell culture processes in this work are described by mathematical process models including well known metabolic links, such as glucose related to lactate production. As shown in previous publications,[3,15,30] the applied model is capable to describe the growth and metabolism of CHO cells in different process conditions and bioreactor scales. It should be noted that this approach is not solely limited to a certain class of mathematical process models and diverse models could be used if they describe the dynamics of cell growth and metabolism, such as hybrid or logistic models.[31,32] To simulate growth and metabolism, adapted mathematical process models, modified from Kuchemüller et al[30,33] and Möller et al[3,15] were used in CS1 and CS2. All calculations and computational methods were performed in MATLAB 2018b.

2.3.1 | Mathematical process model CS1 (GS-CHO)

In CS1, the cell growth (X_t—total cell density, X_d—dead cell density, X_v—viable cell density, see Table S2, Eqs. (3)–(5)) was modeled based on a virtual limiting concentration c_{Ls} (Table S2, Eq. (14)).[34] Due to the altered cell metabolism of the GS-CHO cell line, glutamine (c_{Gln}, Table S2, Eq. (8)) is not only consumed but also formed based on the glutamate (c_{Glt}) uptake (Table S2, Eq. (15)) and the present growth rate μ. The uptake of glucose (c_{Glc}, Table S2, Eq. (7)) and c_{Gln} (Table S2, Eq. (8)) led to the formation of lactate (c_{Lac}, Table S2, Eq. (11)) and ammonia (c_{Amm}, Table S2, Eq. (12)) by glycolysis and glutaminolysis, respectively.[15,35] The cell-specific uptake rates for c_{Glc} and c_{Gln} (Table S2, Eqs. (18)–(19)) were modeled as a function of the current concentration of c_{Glc} and c_{Gln}. Furthermore, a growth-associated term was implemented in Eq. (16) to describe the reduction of the cell-specific uptake rates at lower growth rates.[15] c_{Lac} and c_{Amm} are proportional to c_{Glc} and c_{Gln} uptake ($Y_{Lac/Glc}$ and $Y_{Amm/Gln}$). The uptake of c_{Lac} is described by c_{Glc} lower 0.5 mmol L^{-1}.

The antibody (c_{Ab}, Table S2, Eq. (13)) is expressed constantly and modeled as a function of the cell density.[36] Changes in the working volume (Table S2, Eq. (6)) and concentrations due to sampling and bolus feeding (bolus fed-batch) are also considered in the mass balances. All equations of the mathematical process model can be seen in Table S2.

2.3.2 | Mathematical process model CS2 (CHO DP-12)

The prediction of the cell growth (X_t, X_d, and X_v, Table S3, Eqs. (30)–(32)) was performed based on the main substrates c_{Glc} (Table S3, Eq. (34)) and c_{Gln} (Table S3, Eq. (35)). Changes in the c_{Glc}, c_{Lac} (Table S3, Eq. (36)), c_{Amm} (Table S3, Eq. (37)), c_{Ab} (Table S3, Eq. (38)) and cultivation volume (Table S3, Eq. (33)) were modeled as described in Section 2.3.1. The inhibitory effect of c_{Amm} was considered in the Monod-like structured model (Table S3, Eq. (39)). Equations of the mathematical process model can be seen in Table S3.

2.4 | Quantification of model-parametric uncertainty

The aim of the proposed workflow is the quantification and comparison of the process dynamics in MBR and larger-scale bioreactors. The process dynamics are described by mathematical process models, and the model parametric uncertainty is determined based on the experimental uncertainty. Therefore, the model parameters are adapted repeatedly (1,000 times) and the experimental data is sampled (Monte Carlo sampling, see Figure 1 (1–3)) considering an experimental normally distributed relative error of 5% standard deviation, according to Möller et al[15] and Wechselberger et al[37] (for initial values see Table S4). To adapt the model parameters, the objective function (weighted sum of squared residuals [RSMD]) between the simulated and experimental data for all time points and variables was minimized using the Nelder–Mead algorithm, as commonly used for model parameter identification.[3,22,23,38] Alternative approaches for model parameter identification and adaption are the Bayesian inference method[26,39,54] as well as the adaptive experimental redesign which have been discussed in the past.[40-42] Furthermore, model-based Design of Experiments strategies could be used to design initial experiments and identify suitable model parameters.[43] The RSMD was calculated from the squared difference between the experimental $y_{i,m}$ and simulated value $y_{s,m}$ divided by the number of data points n in the data set (Eq. (1)). k_w is used for weighting individual data points.

$$\mathrm{RMSD} = \sqrt{\sum_{m=1}^{n} \frac{\left(y_{s,m} - y_{i,m}\right)^2}{n} \cdot k_w} \tag{1}$$

Based on the Monte-Carlo sampling and individual adapted model parameters, model parameter probability distributions reflecting the parametric uncertainty can be determined. To evaluate the adapted model parameters and the simulated data, the coefficient of determination R^2 was calculated (Eq. (2)).

$$R^2 = 1 - \frac{\sum_{i=1}^{n} (y_i - y_s)^2}{\sum_{i=1}^{n} (y_i - \bar{y})^2} \tag{2}$$

The R^2 lies between 1 and minus infinity and is defined as the residual of 1 minus the ratio of the squared differences between the experimental-simulated $(y_i - y_s)^2$ as well as the squared differences between the experimental data and their mean $(y_i - \bar{y}_i)^2$. R^2 is equal to 1 if simulated data corresponds to the experimental data measured.[15,44]

2.5 | Statistical comparison of probability distributions

To identify differences in the process dynamics between the two scales, the quantified model parameter distributions are compared statistically using analysis of variance (ANOVA). The p value calculated by the ANOVA function indicates if the difference is significant (α = 1%).[15] Generally, three different significance levels (p values) were chosen (p < 0.001 = highly significant—**, p < 0.01 = significant—*, $p \geq 0.01$ = not significant—n.sig). Subsequently, the means and sample variance were determined for two samples (two model parameter distributions of one model parameter at two scales or experimental setups). The boxplots for each individual model parameter distributions show the 25th and 75th percentile (interquartile distance, bottom and top edges of the box) as well as the upper and lower whiskers covering 99.3% (according to MATLAB preset) of the data set if the data are normally distributed.[45]

2.6 | Monte Carlo-based uncertainty bands

The process variability was simulated based on the former determined model parametric uncertainty. Therefore, uncertainty bands, representing the uncertainty propagation, were determined by calculation of the mean and the 10 and 90% quantiles of each individual model parameter distribution (1,000 simulations with normally distributed standard deviation of 5%) using the function "prctile." Subsequently, simulations with mean, 10 and 90% quantile model parameter values were performed.

2.7 | Transfer of process dynamics

The mathematical transfer was based on the main assumption that the differences in mean and coefficient of variance (CV) are consistent and transferable to cultivation systems with changed experimental

setup, scale or feed constitution. First, mean, standard deviation and CV were determined for all individual model parameter distributions and the differences of these values between two selected systems (e.g., 24-DWP and shake flask, same feed constitution) were calculated. Second, the calculated differences were transferred to an, for example, 24-DWP cultivation system with varying feed constitution. The resulting values for the individual model parameter distributions (i.e., means and standard deviations) were then used as initial values for randomized parameter distributions (1,000 parameter values) of a predicted unknown cultivation system using the randn function in MATLAB. Subsequently, means, standard deviations and CV were determined again.

2.8 | Engineering parameters during scale-up

A matched mixing time approach was used as scaling criterion in CS1. The mixing time for cell cultivations in the micro-matrix and the 5 L bioreactor was roughly 6 s. The mixing time was determined in a pre-experiment by iodine decolorization and additionally verified by the Dual Indicator System for Mixing Time at the UCL (London, UK) for 260 rpm and 3500 ml working volume. In CS2, shaking diameter and frequency were defined according to the manufacturer's protocols.

2.9 | Growth and metabolite analysis

2.9.1 | GS-CHO (CS1)

Cell counts were performed immediately after sampling using a ViCELL XR (Beckman Coulter, UK). The remaining sample volume was centrifuged at 16,100 × *g* for 5 min. The supernatant was analyzed for nutrients, metabolites, and dissolved CO_2 using a Bioprofile FLEX (Nova Biomedical, USA). For both analyzes, samples were diluted with 1×PBS (Life Technologies, UK) where appropriate. The concentration of IgG4 was determined by affinity chromatography using a 1 HiTrap Protein G HP column (GE Healthcare, UK) in combination with an Agilent 1200 (Agilent Technologies, UK) high-performance liquid chromatograph (HPLC).

2.9.2 | CHO DP-12 (CS2)

X_t was determined with the Z2 particle counter (Z2, Beckman Coulter, USA). For further analysis, the cell suspension was centrifuged at 300 × *g* for 3 min and the supernatant was frozen (−20°C). The cell pellet was resuspended in 4°C 1×PBS. The viability of the cells was determined with a DNA staining method (DAPI method). For this, 1 μg ml^{-1} DAPI was added to the cell suspension and measured with a flow cytometer and the 405 nm laser and 450/50 nm (FITC-A) filter signal (CytoFlex, Beckman Coulter, USA). SSC-A versus FSC-A and FSC-H versus FSC-A gating was used to exclude measured cell debris and doublets from non-stained viable cells. Thirty thousand events were recorded in total (CyteExpert Software, Beckman Coulter, USA).

The concentration of c_{Glc}, c_{Gln}, and c_{Lac} concentrations were quantified with a bio-chemistry analyzer (YSI 2900D, Yellow Springs Instruments, USA). c_{Amm} was determined with an enzymatic test kit (AK00091, nzytech, Portugal). The c_{Ab} was measured with bio-layer interferometry (Octet RED, Pall ForteBio, c_{Lac}) with protein A biosensors (Pall ForteBio). All metabolite and product concentrations were measured according to the manufacturer's protocol.

3 | RESULTS AND DISCUSSION

The presented model-based workflow (see Figure 1) was introduced to quantify, compare and potentially transfer the process dynamics between MBR and larger-scale. In CS1, the GS-CHO culture was modeled in the micro-matrix system (MM) and 5 L bioreactor (5 L BR), model-parametric uncertainties were derived and statistically compared. In CS2, model parametric uncertainties and differences in process dynamics between 24-DWP and shake flask culture were determined and compared first. Then, changes in the model parameter distributions were mathematically converted and the bioprocess strategy was transferred to shake flask scale.

3.1 | Model-based scale-up CS1

3.1.1 | Adaptation of model parametric uncertainty (CS1)

As proposed in the model-based workflow (see Figure 1), model parameters of the MM (Section 2.2.1) and 5 L BR (Section 2.2.2) were initially adapted to experimental data by modeling process outcomes and minimizing the RMSD value (Section 2.4). To compare the simulation to the experimental data, individual mean model parameter values were determined and both data sets were displayed in comparison to the simulated data (see Figure 2). Due to missing cultivation data, c_{Gln} was simulated but is not shown in Figure 2. The corresponding time-dependent MM and 5 L BR plots can be seen in Figures S2 and S3. An average goodness of fit R^2 was determined for both data sets (see Section 2.4, Eq. (2)). As can be seen in Figure 2, X_v, X_d, and X_t (Figure 2a–c) were sufficiently simulated by the mean model parameters with R^2 of 0.87 (X_v), 0.67 (X_d), and 0.91 (X_t) for MM and 5 L BR.

Changes in c_{Glc} (Figure 2d) due to sampling and feeding were modeled with high accuracy (R^2 = 0.96). The formation of lactate due to glucose (Figure 2e) consumption was simulated with R^2 = 0.62. At the end of cultivation, the uptake of lactate was underpredicted (see Figures S2 and S3). c_{Amm} (Figure 2f) was modeled with R^2 = -1.07. The uptake and feeding of glutamate (Figure 2g) was simulated with high accuracy (R^2 = 0.91). At the end of the cultivation, slight deviations between the experimental and simulated data occurred. The formation of antibody (Figure 2h) was well described by the model equations and the mean model parameters (R^2 = 0.94). The concentration

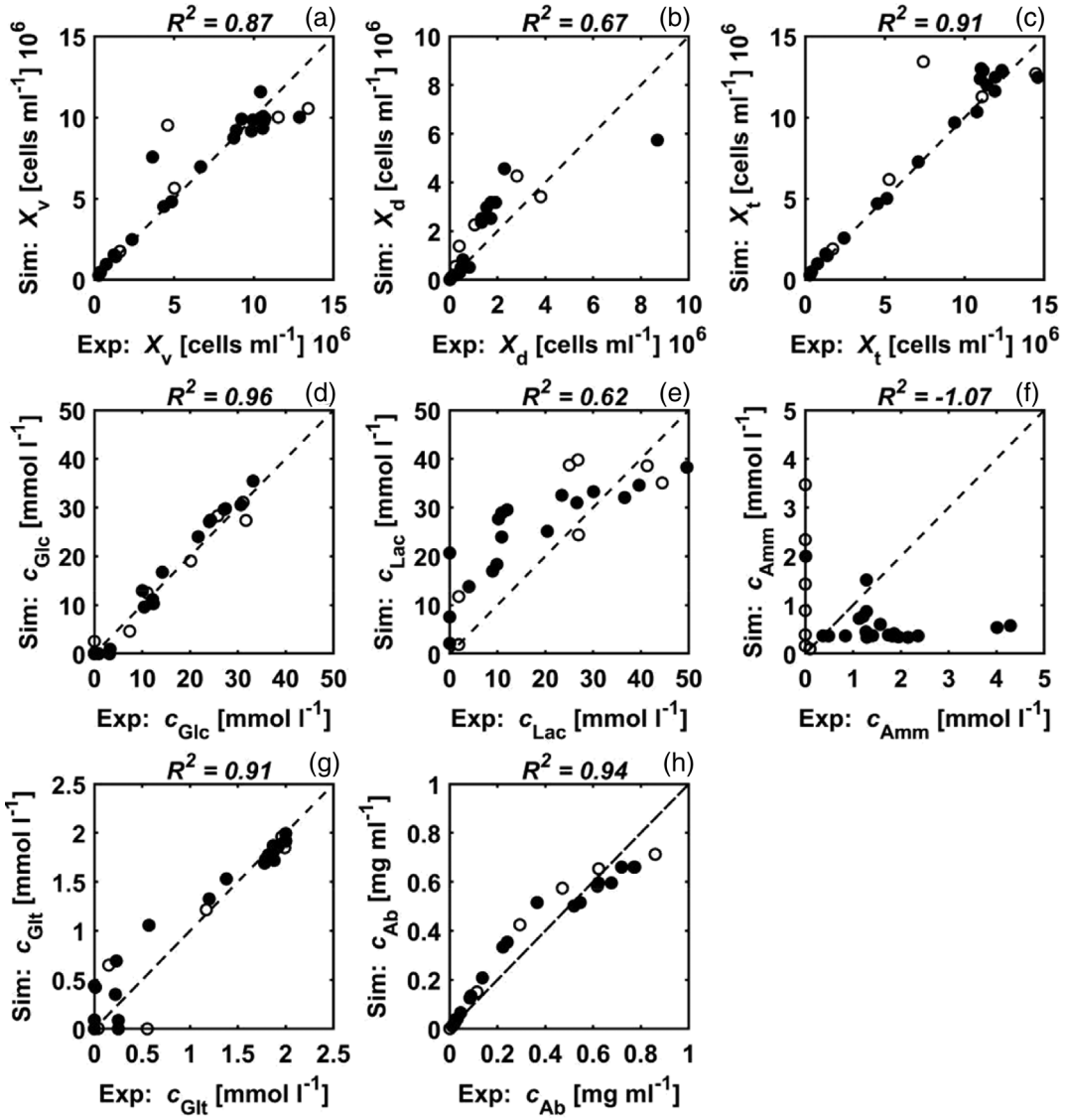

FIGURE 2 Comparison of simulated (Sim:) and experimental data (Exp:) of fed-batch cultivation performed in MM (o) and 5 L BR (•, CS1), n = 1. The goodness of fit is described by R^2 (see Section 2.4, Eq. (2))

of the introduced unknown component c_{Ls} decreased over the cultivation time and reached zero at the end of the cultivation. Changes in the culture volume due to sampling and feeding were calculated (not shown, see Figures S2 and S3).

Overall, cell growth and metabolism of the GS-CHO cell line are sufficiently described at different scales (4 and 3,750 ml, respectively) and the process dynamics can be evaluated by the introduced mathematical process model and the adapted mean model parameters under uncertainty. However, a deeper understanding of the complex cell-specific metabolism, for example, the glutamate and glutamine uptake/formation is necessary as several biological effects are still unknown or difficult to describe. Until now, GS-CHO cell growth and metabolism was modeled in batch and fed-batch cultures by several groups.[46-48] Similar to Xu et al (2019), an unstructured kinetic model rather than a more structured and comprehensive model considering the light and heavy chain formations of the antibody product and extra as well as intracellular fluxes of carbohydrates and amino acids were used.[48] Nevertheless, it can be concluded that this type of the presented unstructured model was sufficient for the prediction of growth and antibody formation.

3.1.2 | Statistical comparison of model parameter distributions MM and 5 L BR (CS1)

To quantify potential differences in the process dynamics between the MM and 5 L BR (as proposed in Figure 1 (4)), the differences in the model parameter distributions resulting from individual model parameter adaptations were initially analyzed by ANOVA (see Figure 1 (3)). For this, 5 out of 17 model parameters were selected based on sensitivity analysis (see Möller et al[15]). Due to the metabolism of GS-CHO cells and the direct correlation of growth and

antibody formation with c_{Glc}, sensitive glucose-related model parameters were selected. First, differences in mean model parameters were calculated and normalized to their starting values (e.g., $\mu_{max,norm}$, see Table S4). Second, the significance value between the calculated differences was determined (see Figure 1 (5)).

As can be seen in Figure 3, small deviations in the mean model parameters between the model parameter distributions of the MM and 5 L BR were quantified for cell metabolism-related model parameters.

The relative mean model parameter values are summarized in Table S5. Model parameter describing the cell growth $\mu_{max,norm}$ and the antibody formation rate $q_{Ab,max,norm}$ did not change significantly. This is confirmed by similar maximal X_v (12.9×10^6 and 13.4×10^6 cells ml^{-1} after 220 and 213 h, respectively) and c_{Ab} (0.77 and 0.86 g L^{-1} after 345 and 316 h, respectively) in both bioreactor systems. Significant differences were identified for glucose-related model parameters. $K_{Glc,norm}$ was 56.8% lower, $K_{S,Glc,norm}$ 10.6% higher and $q_{Glc,max,norm}$ 45.4% higher in the 5 L BR. Compared to the 5 L BR, the total working volume was kept constant in the MM and feeding volume was adjusted accordingly to different sample volumes (see Figure S2). The central metabolism of mammalian cell lines is complex and flexible due to deregulation[2] and adaption of the central metabolism to changing extracellular substrate concentrations or heterogeneities in the bioreactor system[35,49,50] which could led to changes in $K_{S,Glc,norm}$, $K_{Glc,norm}$, and $q_{Glc,max,norm}$ mean in the MM and 5 L BR.

Overall, the model parameter distributions of the MM and 5 L BR showed only marginally significant differences (see Figure 1 (6)) in the glucose metabolism with obviously no influence on the bioprocess dynamics. Furthermore, no differences were present for cell growth and antibody formation. Therefore, under consideration of model parametric uncertainties, it can be concluded that the growth and product formation were the same in both bioreactor systems and that the MM reflected the process dynamics of the 5 L BR (see Figure 1 (9)). Thus, no mathematical conversion and transfer of the process dynamics (see Figure 1 (8)) was needed and the MM can be considered as a suitable scale-down device in terms of cell growth and product formation.

3.2 | Model-based scale-up CS2

3.2.1 | Adaptation of model parametric uncertainty DWP Feed A and SF Feed A (CS2)

According to the proposed model-based workflow (see Figure 1), changes in the process dynamics due to different scales should be quantified and evaluated for the 24-DWP (referred as DWP Feed A and DWP Feed B) and shake flask culture with Feed A (referred as SF Feed A) (see Figure 1 (1 and 2)). The simulated and experimental data of DWP Feed B as well as time-dependent plots are shown in Figures S1 and S4. As shown in Figure 4a–c, X_v, X_d, and X_t were sufficiently simulated by the mean model parameter values with R^2 = 0.72 (X_v), 0.40 (X_d), and 0.88 (X_t).

The consumption of glucose (Figure 4d) and glutamine (Figure 4e) as well as changes in the concentrations due to feeding and sampling of medium was modeled accurately and were comparable to Möller et al.[15] Deviations can be mainly attributed to the over-predicted cell densities at the end of the cultivation. The progression of c_{Lac} (Figure 4f) was predicted precisely until 72 h and then over-predicted (R^2 = -12.1). After 72 h, c_{Lac} increase declined and a constant c_{Lac} was

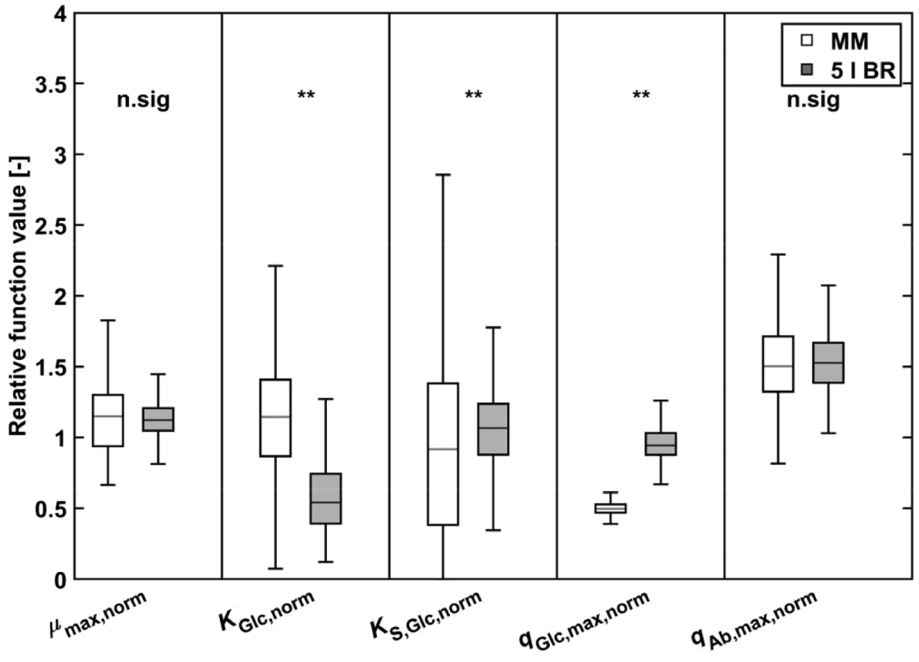

FIGURE 3 Boxplots of normalized model parameters of fed-batch cultivation MM and BR (CS1). The intrinsic distribution of 1,000 independent model parameter estimations is displayed per box. All model parameters are normalized to their individual starting value during model parameter estimation (see Tables S4 and S5). n.sig, not significant ($p \geq 0.01$); *, significant ($p < 0.01$); **, highly significant ($p < 0.001$)

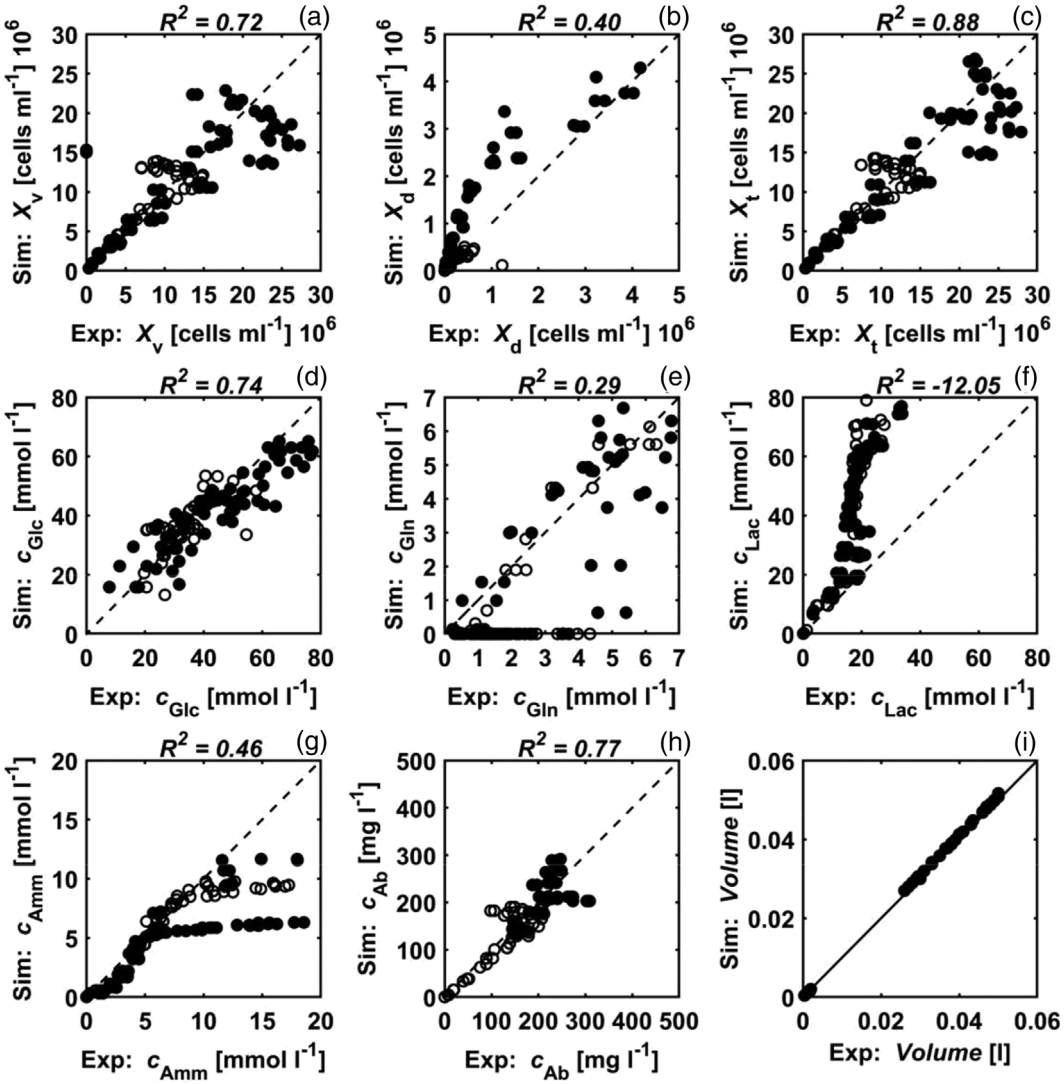

FIGURE 4 Comparison of simulated (Sim:) and experimental data (Exp:) of 4 fed-batch cultivations performed in 24-DWP with Feed A (o) and shake flask with Feed A (•, CS2). The goodness of fit is described by R^2 (see Section 2.4, Eq. (2))

observed. The experimental and simulated concentration profiles can be seen in the time-dependent plots (see Figures S4 and S5). This effect is part of a different research study focusing on the metabolic regulation of the pyruvate dehydrogenase complex and its role during the lactate switch.[51] Until 120 h, c_{Amm} (Figure 4g) was modeled well but due to underpredicted c_{Gln}, c_{Amm} was underpredicted as well (R^2 = 0.46). The course of c_{Ab} (Figure 4h) was modeled with good accuracy and was associated with the progression of the viable cell density (R^2 = 0.77). Changes in the culture volume (Figure 4i) because of sampling, feeding and evaporation of medium were calculated.

Overall, the growth and product formation as well as the dynamics in the 24-DWP with the two different constituted Feeds A and B (see Figure S1) and shake flask with Feed A were simulated and reflected sufficiently by the introduced model and mean model parameters at different scales (2 and 30 ml working volume, respectively) and under experimental uncertainty. However, similar to CS1, deeper insights into the complex metabolism under substrate limitation and cellular regulations are necessary to further reduce deviations.

3.2.2 | Statistical comparison of model parameter distributions DWP Feed A and SF Feed A (CS2)

Similar to CS1 and suggested in the workflow (Figure 1), changes in the process dynamics between the DWP and shake flask culture due to different scales are analyzed by ANOVA (see Figure 1 (3)). Subsequently, the differences in the model parameter distributions resulting from individual parameter estimations are quantified (see Figure 1 (4)). The mean model parameter values are summarized in Table S5. As in Section 3.1.2 the individual model parameter distributions of the sensitive model parameters (see Möller et al[15]) are compared and tested for significance (Figure 1 (5)). In contrast to CS1, glutamine-related model parameters were considered as more relevant in CS2 due to the

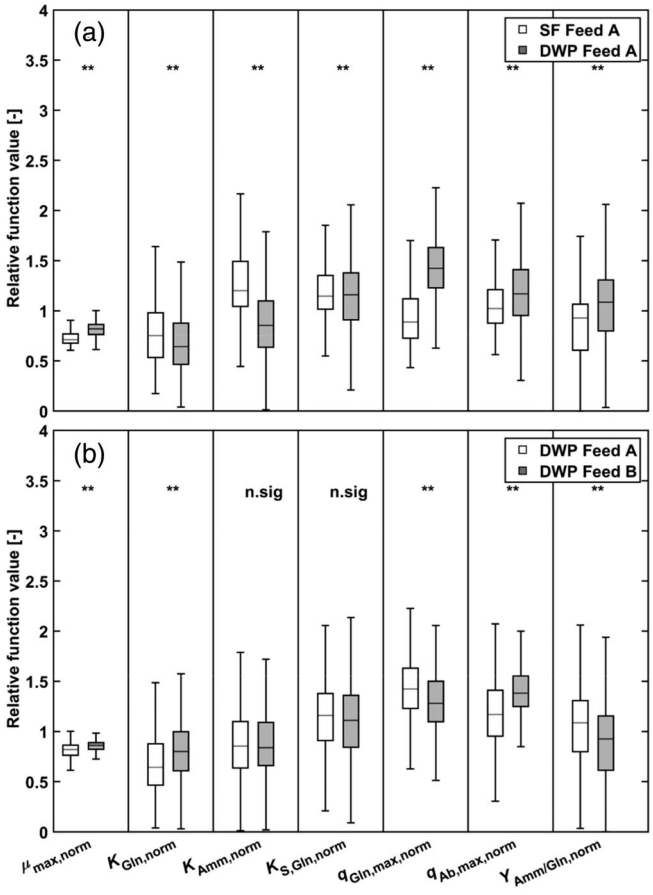

FIGURE 5 (a) Comparison of fed-batch cultivations DWP Feed A and SF Feed A (CS2). (b) Comparison of fed-batch cultivations DWP Feed A and DWP Feed B (CS2). Boxplots of normalized model parameters. The intrinsic distribution of 1000 independent model parameter estimations is displayed per box. All model parameters are normalized to their individual starting value during model parameter estimation (see Tables S4 and S5). n.sig, not significant ($p \geq 0.01$); *, significant ($p < 0.01$); **, highly significant ($p < 0.001$)

metabolism of the CHO DP-12 cells. For the model parameter distributions of SF and DWP with Feed A, seven significantly different model parameter distributions with varying mean model parameter value were identified, as can be seen in Figure 5a.

As indicated by the location of the median and interquartile distance of the boxplots, all investigated model parameter distributions changed for growth- and metabolism-related model parameters. Highly significant differences (**) were identified for all sensitive model parameters between SF Feed A and DWP Feed A. The growth-related mean model parameter values of $\mu_{max,norm}$ increased by 11.1% and $K_{S,Gln,norm}$ decreased by 5.5% for DWP Feed A. Compared to SF Feed A, $K_{Gln,norm}$ decreased by 7.5% and $K_{Amm,norm}$ by 45.7% whereas the model parameter values of $q_{Gln,max,norm}$ (35.1%), $q_{Ab,max,norm}$ (13.3%), and $Y_{Amm/Gln,norm}$ (22.3%) increased for DWP A. These differences can be directly related to higher X_v (27.3×10^6 cells ml^{-1} compared to 14.9×10^6 cells ml^{-1} after 168 h for SF and DWP Feed A, see Table 1) and changed metabolic profile (see Figures 4, S4 and S5). Mora et al reported differences in growth and protein expression for dhfr-deficient CHO cells in 24-DWP and conventional shake flask cultures which can be mainly attributed to changes in the physical culture conditions.[52] The decrease in $q_{Gln,max,norm}$ for SF Feed A can be related to different c_{Gln} profiles and thus changes in the process dynamics which are reflected by the process model. Compared to DWP Feed A, simulated and experimental c_{Gln} deviated more for SF Feed A and the c_{Gln} reached 0 mmol L^{-1} after 144 h whereas a concentration of 1.3 mmol L^{-1} was measured after 264 h (see Figures S4 and S5). For SF Feed A higher $K_{Amm,norm}$ values were obtained due to higher c_{Ab} (0.42 g L^{-1} compared to 0.21 g L^{-1} for DWP Feed A after 213 h, see Table S1) at the end of cultivation and the use of $K_{Amm,norm}$ as boundary condition for antibody formation (see Table S3, Eq. (23)).

It can be concluded that between different bioreactor scales physical process conditions and process dynamics changed for DWP Feed A and SF Feed A (see Figure 1 (7)). These differences can be reflected by significant changes in the model parameter distributions of growth-associated as well as product formation-associated model parameters. The histograms of the corresponding model parameter distributions (see Figures S9 and S11) showed normal distribution and reflected the parametric uncertainty based on the experimental variation. According to the proposed workflow, a mathematical conversion of the determined differences (Figure 1 (8)) and transfer of the process strategy (Figure 1 (9)) between the scales should be performed.

3.2.3 | Mathematical conversion of model parameter distributions DWP Feed A and SF Feed A (CS2)

The differences in means, standard deviations, and CV of the individual model parameter distributions between DWP Feed A and SF Feed

Model parameter	Mean DWP Feed A	Mean SF Feed A	Δ	Unit
μ_{max}	0.0409	0.0363	0.0045	(h^{-1})
K_{Gln}	1.0634	1.1432	0.0798	(mmol L^{-1})
K_{Amm}	10.965	15.978	5.0132	(mmol L^{-1})
$K_{S,Gln}$	0.0344	0.0363	0.0019	(mmol L^{-1})
$q_{Gln,max}$	4.36×10^{-11}	2.83×10^{-11}	1.53×10^{-11}	(mmol (cell h)$^{-1}$)
$q_{Ab,max}$	3.04×10^{-10}	2.64×10^{-10}	4.04×10^{-11}	(mmol (cell h)$^{-1}$)
$Y_{Amm/Gln}$	1.0479	0.8145	0.2334	(–)

TABLE 2 Mathematical conversion mean model parameter distributions DWP Feed A and SF Feed A (CS2)

A were calculated as described in Section 2.7. Calculated mean values of the sensitive model parameters are summarized in Table 2.

3.2.4 | Statistical comparison of model parameter distributions DWP Feeds A and B (CS2)

As a consequence of differences between DWP Feed A and SF Feed A (see Section 3.2.2) and thus process dynamics, differences due to varying feed constitutions (Feeds A and B) should be investigated in MBR-scale.

Significance between the mean model parameter values of DWP Feeds A and B were identified for 5 out of 7 sensitive model parameters (see part B Figure 5). An increase of 4.5% was determined for the maximum cell specific growth rate $\mu_{max,norm}$ for DWP Feed B, directly influencing cell growth. These differences were confirmed by higher final viable cell densities (X_v of 19.2×10^6 cells ml^{-1} after 192 h compared to 13.1×10^6 cells ml^{-1} after 162 h for DWP Feeds A and B, respectively). Model parameters influencing glutamine uptake ($K_{Gln,norm}$ and $q_{Gln,max,norm}$) changed significantly (**), which was confirmed by slightly different c_{Gln} profiles (see Figure S4). Besides, antibody formation rate $q_{Ab,max,norm}$ (**, direct association of growth and antibody formation, c_{Ab} of 0.17 and 0.30 g L^{-1} after 213 and 264 h for DWP Feeds A and B, respectively, see Table 1, setup 1) increased by 16.3% and $Y_{Amm/Gln,norm}$ (**) decreased by 16.4% (**) for DWP Feed B. $K_{Amm,norm}$ and $K_{S,Gln,norm}$ did not changed significantly (n.sig). In summary, differences in the process dynamics of the growth and metabolism were determined and evaluated between DWP Feed A and SF Feed A as well as DWP Feeds A and B. Thus, changes in dynamics due to varying feed constitution and bioreactor scales can be reflected by the introduced process model and changed individual model parameter distributions. The quantified differences in mean and variance of the individual model parameter distributions (DWP Feeds A and B) will be used to transfer the process dynamics of the MBR system to a cultivation system in development scale (i.e., shake flask) with unknown process outcomes as proposed in the workflow (see Figure 1 (7–9)).

TABLE 3 Information transfer for the prediction of μ_{max} for an unknown cultivation system (CS2)

Cultivation system	Mean μ_{max} (h^{-1})	(h^{-1})	CV (–)
DWP Feed A	0.0409	0.0044	0.11
DWP Feed B	0.0427	0.0026	0.06
SF Feed A	0.0363	0.0031	0.086
SF Feed B	0.0382	0.0015	0.041

3.2.5 | Transfer of process dynamics (CS2)

Based on the differences in the process dynamics between 24-DWP- and shake flask scale and varying feed constitution, the mathematical conversion of the dynamics and the information transfer (see Figure 1 (8)) was performed to quantify an unknown cultivation system and enable scale-up (see Figure 1 (9)). Therefore, differences in mean, CV and standard deviation were calculated, that is, between DWP Feeds A and B, and then transferred to the unknown system, that is, SF Feed B (shake flask culture with Feed B). In Table 3, the change in the mean value of μ_{max} after the information transfer is exemplarily shown.

Significant (*) and highly significant differences (**) were identified for all model parameters except $K_{Amm,norm}$ and $K_{S,Gln,norm}$. The interquartile distance, location of the median and whisker length of the boxplots varied (Figure S6).

Simulation of predicted cultivation (CS2) with the estimated mean model parameter values, a shake flask fed-batch cultivation with initial Feed B feeding after 48 h was simulated. The progression of the simulated cell density and product concentration as well as the experimental data of the validation experiment (as described in Table S1) can be seen in Figure 6.

The course of the X_v (Figure 6a) was simulated accurately by the mathematically converted and transferred model parameters from DWP- to shake flask scale (within uncertainty bands). c_{Ab} (Figure 6b)

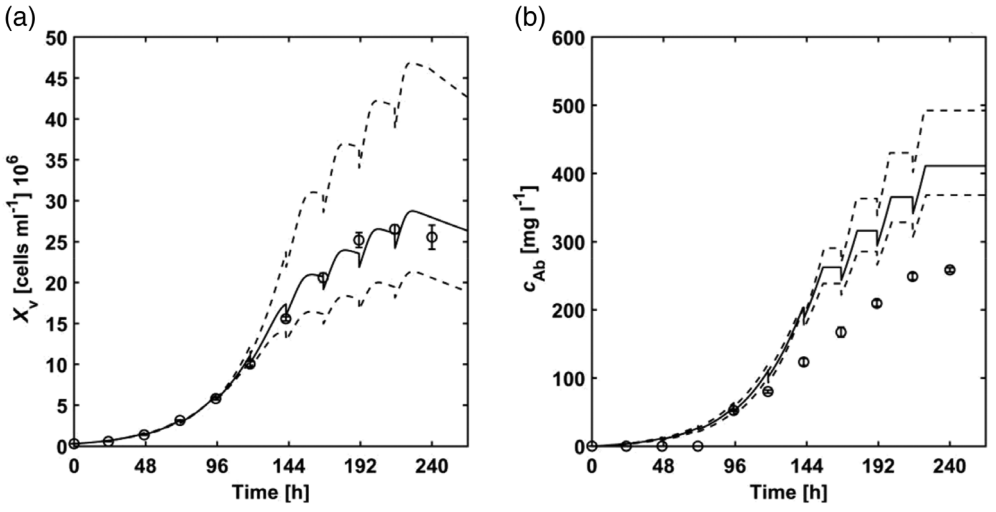

FIGURE 6 Simulated (–) and experimental data (o) for SF Feed B fed-batch cultivation and validation experiment performed in shake flask culture (30–50 ml, CS2) and feeding after 48 h. The dotted lines represent the 10% and 90% quantiles based on the model parameter distributions. Average values were used (n = 4)

was simulated qualitatively but over-predicted (outside the uncertainty bands). The maximal X_v of 26.5 ± 0.5 × 10^6 cells ml^{-1} and c_{Ab} of 0.26 ± 0.003 g L^{-1} was measured after 216 and 240 h, respectively. Compared to DWP Feed A, DWP Feed B and SF Feed A (all validation experiments) the X_v increased by 95%, 47% and 53%, respectively. The maximum c_{Ab} (Figure 6b) increased by 82 and 75% compared to DWP Feed A and SF Feed A validation experiments, respectively, but was similar to the final concentration of the DWP Feed B cultivation. The over-prediction of the product titer mainly resulted from high antibody formation rates q_{Ab} and the direct relation to the X_v. The antibody formation for CHO DP-12 cells was found to be dependent on a variety of different effects, for example, subpopulation formation,[53] cell-cycle-dependent metabolic regulations (i.e., regulation of pyruvate dehydrogenase complex) and so far, not well identified effects.[23]

4 | CONCLUSION

In this work, a model-based workflow for the scale-up of a process strategy developed in MBR- to larger scale as well as evaluation and comparison of the process dynamics was introduced. The dynamics are described by mathematical process models and model parameters determined under consideration of experimental variability. Based on the model parameter probability distributions generated for different bioreactor scales and media constitutions, differences in the dynamics were quantified. The model-based workflow was discussed for two different case studies. On the one hand side, it was shown that process dynamics of a GS-CHO cell line in a micro-matrix and commonly used 5 L bioreactor system are comparable based on the evaluated growth- and product-related model parameter distributions. This confirmed the main assumption of similar process conditions in the MM and 5 L BR. On the other hand side, a 24-DWP and shake flask culture showed significant differences in the model parameter distributions influencing the bioprocess dynamics. According to the workflow, changes were mathematically converted and model outcomes of an unknown cultivation at shake flask scale were simulated adequately. Thus, the proposed workflow can be sufficiently used to scale-up process strategies from small to larger scale for a more knowledge-driven decision making. Beside the scale-up application, MBRs and the workflow are also applicable for the evaluation of scale-down approaches. Additional studies will focus on the automated conduction of manually performed parts of the workflow and the coupling of computational fluid dynamics with mathematical process models. The combination of this workflow with advanced analytical tools may be beneficial to capture fast changes in the process dynamics and identify so far unknown effects.[24]

NOTATION

ABBREVIATION

24-DWP	24-Deep-Well-Plate
Ab	antibody
Amm	ammonium
ANOVA	analysis of variance
BR	bioreactor
CHO	Chinese hamster ovary
CS	case study
CV	coefficient of variation
DAPI	4′,6-diamidino-2-phenylindole
Feed A/B	feed medium A/B
FITC-A	fluorescein isothiocyanate filter in flow cytometry
FSC	forward scatter
Glc	glucose
Gln	glutamine
Glt	glutamate
GS-CHO	glutamine synthetase Chinese hamster ovary
Lac	lactate
LHS	Latin-Hypercube sampling
MBR	miniaturized bioreactor
MM	micro-matrix
PBS	phosphate-buffered saline
QbD	Quality by Design
RMSD	root mean square deviation
SF	shake flask
STR	stirred tank reactor

NOMENCLATURE

p	significance level (–)
c_i	concentration of the component i (mmol L^{-1})
$c_{i,0}$	initial concentration fed-batch (mmol L^{-1})
F_i	concentration of component i in feed (mmol L^{-1})
F_{Start}	time, start of feed (h)
F_{End}	time, end of feed (h)
F_{points}	number of feed points (–)
F_V	feed volume (ml h^{-1})
k_d	cell-specific death rate (h^{-1})
K_i	kinetic constant (mmol L^{-1})
k_{Lys}	cell-specific lyse rate (h^{-1})
$K_{S,i}$	Monod constant (mmol L^{-1})
k_w	weighting factor (–)
i	cell-specific growth rate (h^{-1})
n	number of data points (–)
p	significance factor (–)
q_i	substrate-specific uptake and formation rate (mmol (cell h)$^{-1}$)
R^2	coefficient of determination (–)
rpm	rounds per minute (min^{-1})
σ	standard deviation (h^{-1})
t	time (h)
V_i	reactor volume (ml)
X_d	death cell density (cells L^{-1})

X_t	total cell density (cells L^{-1})
X_v	viable cell density (cells L^{-1})
$Y_{i,j}$	yield coefficient (–)
y_i	experimental value (–)
$\bar{y}_i$	Mean experimental value (–)
y_s	simulated value (–)
vvm	volumetric aeration rate (min^{-1})

ACKNOWLEDGMENT

We thank Tanja Hernández Rodríguez (Ostwestfalen-Lippe University of Applied Sciences and Arts, Biotechnology and Bioprocess Engineering) for feedback on statistical tools. Open Access funding enabled and organized by ProjektDEAL.

CONFLICT OF INTEREST

The authors declare that there are no conflicts of interest.

AUTHOR CONTRIBUTION

All authors contributed to the paper. All authors have read and agreed to the published version of the manuscript.

DATA AVAILABILITY STATEMENT

The data that support the findings of this study are available from the corresponding author upon reasonable request.

ORCID

Ralf Pörtner https://orcid.org/0000-0003-1163-9718
Johannes Möller https://orcid.org/0000-0001-9546-055X

REFERENCES

1. Betts JPJ, Warr SRC, Finka GB, et al. Impact of aeration strategies on fed-batch cell culture kinetics in a single-use 24-well miniature bioreactor. *Biochem Eng J*. 2014;82:105-116.
2. Eibl R, Eibl D, Pörtner R, Catapano G, Czermak P. *Cell and Tissue Reaction Engineering*. Berlin Germany: Springer Science; 2008.
3. Möller J, Kuchemüller KB, Steinmetz T, Koopmann KS, Pörtner R. Model-assisted design of experiments as a concept for knowledge-based bioprocess development. *Bioprocess Biosyst Eng*. 2019;42:867-882.
4. Betts JI, Doig SD, Baganz F. Characterization and application of a miniature 10 mL stirred-tank bioreactor, showing scale-down equivalence with a conventional 7 L reactor. *Biotechnol Prog*. 2006;22:681-688.
5. Chaturvedi K, Sun SY, OBrien T, Liu YJ, Brooks JW. Comparison of the behavior of CHO cells during cultivation in 24-square deep well microplates and conventional shake flask systems. *Biotechnol Reports*. 2014;1-2:22-26.
6. Gernaey KV, Baganz F, Franco-Lara E, et al. Monitoring and control of microbioreactors: an expert opinion on development needs. *Biotechnol J*. 2012;7:1308-1314.
7. Lye GJ, Ayazi-Shamlou P, Baganz F, Dalby PA, Woodley JM. Accelerated design of bioconversion processes using automated microscale processing techniques. *Trends Biotechnol*. 2003;21:29-37.
8. Micheletti M, Barrett T, Doig SD, et al. Fluid mixing in shaken bioreactors: implications for scale-up predictions from microlitre-scale microbial and mammalian cell cultures. *Chem Eng Sci*. 2006;61:2939-2949.
9. Rouiller Y, Perilleux A, Collet N, Jordan M, Stettler M, Broly H. A high-throughput media design approach for high performance mammalian fed-batch cultures. *MAbs*. Vol 5. New York, United States: Taylor & Francis; 2013:501-511.
10. Wiegmann V, Giaka M, Martinez CB, Baganz F. Towards the development of automated fed-batch cell culture processes at microscale. *Biotechniques*. 2019;67:238-241.
11. Barrett TA, Wu A, Zhang H, Levy MS, Lye GJ. Microwell engineering characterization for mammalian cell culture process development. *Biotechnol Bioeng*. 2010;105:260-275.
12. Girard P, Meissner P, Jordan M, Tsao M, Wurm FM. Small scale bioreactor system for process development and optimization. *Animal Cell Technology: Products from Cells, Cells as Products*. Dordrecht, The Netherlands: Springer; 1999:323-327.
13. Silk NJ, Denby S, Lewis G, et al. Fed-batch operation of an industrial cell culture process in shaken microwells. *Biotechnol Lett*. 2010;32:73-78.
14. Wolf MKF, Lorenz V, Karst DJ, Souquet J, Broly H, Morbidelli M. Development of a shake tube-based scale-down model for perfusion cultures. *Biotechnol Bioeng*. 2018;115:2703-2713.
15. Möller J, Hernandez Rodriguez T, Müller J, et al. Model uncertainty-based evaluation of process strategies during scale-up of biopharmaceutical processes. *Comput Chem Eng*. 2020;134:106693.
16. Neubauer P, Cruz N, Glauche F, Junne S, Knepper A, Raven M. Consistent development of bioprocesses from microliter cultures to the industrial scale. *Eng Life Sci*. 2013;13:224-238.
17. Delvigne F, Takors R, Mudde R, Gulik W, Noorman H. Bioprocess scale-up/down as integrative enabling technology: from fluid mechanics to systems biology and beyond. *J Microbial Biotechnol*. 2017;10:1267-1274.
18. Ferreira AP, Tobyn M. Multivariate analysis in the pharmaceutical industry: enabling process understanding and improvement in the PAT and QbD era. *Pharm Dev Technol*. 2015;20:513-527.
19. Patil AS, Pethe AM. Quality by design (QbD): a new concept for development of quality pharmaceuticals. *Int J Pharmaceut Qual Assur*. 2013;7:13-19.
20. Rathore AS. Roadmap for implementation of quality by design (QbD) for biotechnology products. *Trends Biotechnol*. 2009;27:546-553.
21. Sin G, Gernaey KV, Lantz AE. Good modeling practice for PAT applications: propagation of input uncertainty and sensitivity analysis. *Biotechnol Prog*. 2009;25:1043-1053.
22. Kroll P, Hofer A, Ulonska S, Kager J, Herwig C. Model-based methods in the biopharmaceutical process lifecycle. *Pharm Res*. 2017;34:2596-2613.
23. Möller J, Korte K, Pörtner R, Zeng AP, Jandt U. Model-based identification of cell-cycle-dependent metabolism and putative autocrine effects in antibody producing CHO cell culture. *Biotechnol Bioeng*. 2018;115:2996-3008.
24. Möller J, Bhat K, Riecken K, Pörtner R, Zeng AP, Jandt U. Process-induced cell cycle oscillations in CHO cultures: online monitoring and model-based investigation. *Biotechnol Bioeng*. 2019;116:2931-2943.
25. Narayanan H, Luna MF, Stosch M, et al. Bioprocessing in the digital age: the role of process models. *Biotechnol J*. 2020;15:1900172.
26. Hernandez Rodriguez T, Posch C, Schmutzhard J, et al. Predicting industrial scale cell culture seed trains - a Bayesian framework for model fitting and parameter estimation, dealing with uncertainty in measurements and model parameters, applied to a nonlinear kinetic cell culture model, using a MCMC method. *Biotechnol Bioeng*. 2019;116:2944-2959.
27. Anane E, Garc a AC, Haby B, et al. A model-based framework for parallel scale-down fed-batch cultivations in mini-bioreactors for accelerated phenotyping. *Biotechnol Bioeng*. 2019;116:2906-2918.
28. Zahel T, Hauer S, Mueller EM, et al. Integrated process modeling: a process validation life cycle companion. *Bioengineering*. 2017;4:86.
29. Duetz WA, Witholt B. Oxygen transfer by orbital shaking of square vessels and deepwell microtiter plates of various dimensions. *Biochem Eng J*. 2004;17:181-185.

30. Kuchemüller KB, Pörtner R, Möller J. Efficient Optimization of Process Strategies with Model-Assisted Design of Experiments.235–249. New York, NY: Springer US 2020.
31. Glassey J. Hybrid modeling of pharmaceutical processes and process analytical technologies. *Hybrid Modeling in Process Industries*. New York, United States: CRC Press; 2018:191-212.
32. Xu P. Analytical solution for a hybrid logistic-Monod cell growth model in batch and continuous stirred tank reactor culture. *Biotechnol Bioeng*. 2020;117:873-878.
33. Kuchemüller KB, Pörtner R, Möller J. Digital twins and their role in model-assisted design of experiments. *Anal Bioanal Chem*. 2020: 1-33.
34. Frahm B, Lane P, Märkl H, Pörtner R. Improvement of a mammalian cell culture process by adaptive, model-based dialysis fed-batch cultivation and suppression of apoptosis. *Bioprocess Biosyst Eng*. 2003;26: 1-10.
35. Ozturk S, Hu WS. *Cell Culture Technology for Pharmaceutical and Cell-Based Therapies*. New York, United States: CRC Press; 2005.
36. Frahm B, Lane P, Atzert H, et al. Adaptive, model-based control by the open-loop-feedback-optimal (OLFO) controller for the effective fed-batch cultivation of hybridoma cells. *Biotechnol Prog*. 2002;18: 1095-1103.
37. Wechselberger P, Sagmeister P, Herwig C. Model-based analysis on the extractability of information from data in dynamic fed-batch experiments. *Biotechnol Prog*. 2013;29:285-296.
38. Nelder JA. Mead R. a simplex method for function minimization. *Comput J*. 1965;7:308-313.
39. Moser A, Kuchemüller KB, Sahar D, et al. Model-assisted DoE software: optimization of growth and biocatalysis in *Saccharomyces cerevisiae* bioprocesses. *Bioprocess Biosyst Eng*. 2020.
40. Barz T, Korkel S, Wozny G, Lopez Cardenas DC. Nonlinear ill-posed problem analysis in model-based parameter estimation and experimental design. *Comput Chem Eng*. 2015;77:24-42.
41. Barz T, Sommer A, Wilms T, Neubauer P, Bournazou MNC. Adaptive optimal operation of a parallel robotic liquid handling station. *IFAC-PapersOnLine*. 2018;51:765-770.
42. Cruz Bournazou MN, Barz T, Nickel DB, et al. Online optimal experimental re-design in robotic parallel fed-batch cultivation facilities. *Biotechnol Bioeng*. 2017;114:610-619.
43. Abt V, Barz T, Cruz-Bournazou MN, et al. Model-based tools for optimal experiments in bioprocess engineering. *Curr Opin Chem Eng*. 2018;22:244-252.
44. Cameron AC, Windmeijer FAG. An R-squared measure of goodness of fit for some common nonlinear regression models. *J Econometr*. 1997;77:329-342.
45. Langford E. Quartiles in elementary statistics. *J Statist Educ*. 2006;14.
46. McLeod J, O'Callaghan PM, Pybus LP, et al. An empirical modeling platform to evaluate the relative control discrete CHO cell synthetic processes exert over recombinant monoclonal antibody production process titer. *Biotechnol Bioeng*. 2011;108:2193-2204.
47. Niu H, Amribt Z, Fickers P, Tan W, Bogaerts P. Metabolic pathway analysis and reduction for mammalian cell cultures: towards macroscopic modeling. *Chem Eng Sci*. 2013;102:461-473.
48. Xu J, Tang P, Yongky A, et al. Systematic development of temperature shift strategies for Chinese hamster ovary cells based on short duration cultures and kinetic modeling. *MAbs*. 2019;11:191-204.30230966.
49. Lara AR, Galindo E, Ramirez OT, Palomares LA. Living with heterogeneities in bioreactors. *Mol Biotechnol*. 2006;34:355-381.
50. Wang G, Tang W, Xia J, Chu J, Noorman H, Gulik WM. Integration of microbial kinetics and fluid dynamics toward model-driven scale-up of industrial bioprocesses. *Eng Life Sci*. 2015;15:20-29.
51. Möller J, Bhat K, Guhl L, Pörtner R, Jandt U, Zeng AP. Regulation of pyruvate dehydrogenase complex related to lactate switch in CHO cells. *Eng Life Sci*. 2020.
52. Mora A, Zhang S, Carson G, Nabiswa B, Hossler P, Yoon S. Sustaining an efficient and effective CHO cell line development platform by incorporation of 24-deep well plate screening and multivariate analysis. *Biotechnol Prog*. 2018;34:175-186.
53. Möller J, Rosenberg M, Riecken K, Pörtner R, Zeng AP, Jandt U. Quantification of the dynamics of population heterogeneities in CHO cultures with stably integrated fluorescent markers. *Anal Bioanal Chem*. 2020;412:2065-2080.
54. Hernández Rodríguez T, Posch C, Pörtner R, Frahm B. Dynamic parameter estimation and prediction over consecutive scales, based on moving horizon estimation: applied to an industrial cell culture seed train. *Bioprocess and Biosystems Engineering*. 2020. http://dx.doi.org/10.1007/s00449-020-02488-1.

SUPPORTING INFORMATION

Additional supporting information may be found online in the Supporting Information section at the end of this article.

How to cite this article: Arndt L, Wiegmann V, Kuchemüller KB, Baganz F, Pörtner R, Möller J. Model-based workflow for scale-up of process strategies developed in miniaturized bioreactor systems. *Biotechnol Progress*. 2021;37: e3122. https://doi.org/10.1002/btpr.3122